The United Nations University

GEOTHERMAL TRAINING PROGRAMME
Orkustofnun, Grensásvegur 9,
IS-108 Reykjavík, Iceland

Reports 2000
Number 9

GEOCHEMICAL CHARACTERISTICS OF THE GREATER OLKARIA GEOTHERMAL FIELD, KENYA

Cyrus W. Karingithi
Kenya Electricity Generating Co Ltd,
Olkaria Geothermal Project,
P. O. Box 785, Naivasha,
KENYA
ckaringithi@kengen.co.ke

ABSTRACT

Aquifer fluid compositions and aqueous species distribution have been calculated for samples from nineteen wells in the greater Olkaria high-temperature geothermal field, Kenya, with the aid of the WATCH-speciation program. It is concluded that overall mineral-solution equilibrium is closely approached at quartz equilibrium temperature with respect to most hydrothermal minerals occurring in the aquifer. The minerals involved are in alphabetical order: albite, anhydrite, calcite, epidote, fluorite, microcline, prehnite, pyrite and pyrrhotite.

The solute geothermometers indicate temperatures similar to anticipated aquifer temperatures. However, the gas geothermometers give temperatures either higher or lower than measured aquifer temperatures. The chemical composition of the alteration minerals of the buffer participating in the gas equilibrium is required to formulate new calibration that will be suitable or appropriate for the Olkaria geothermal field discharges. The stable water isotopes indicate that the fluid discharged in the eastern and western fields has different sources.

1. INTRODUCTION

The Greater Olkaria geothermal area (GOGA) is located in the central sector of the Kenya Rift Valley to the south of Lake Naivasha and 120 km northwest of Nairobi (Figure 1). The Kenya Rift Valley is an integral part of the East African Rift Valley system, which extends for over 3000 km from southern Mozambique through Tanzania, Kenya and Ethiopia to join the Red Sea and the Gulf of Aden rifts at the Afar triple junction (KenGen, 1998). The Olkaria high-temperature geothermal field is associated with a region of Quaternary volcanism. Twelve similar Quaternary volcanic centres occur in the axial region of the rift and are potential geothermal resources (Omenda, 1998; Omenda et al., 1993; Riaroh and Okoth, 1994).

Exploration for geothermal energy started in the early 1950s when two wells were drilled at Olkaria. Between 1960 and 1970 a lot of surface exploration work was carried out in the Central Rift Valley through the UNDP (United Nations Development Programme) and the Kenya Government through

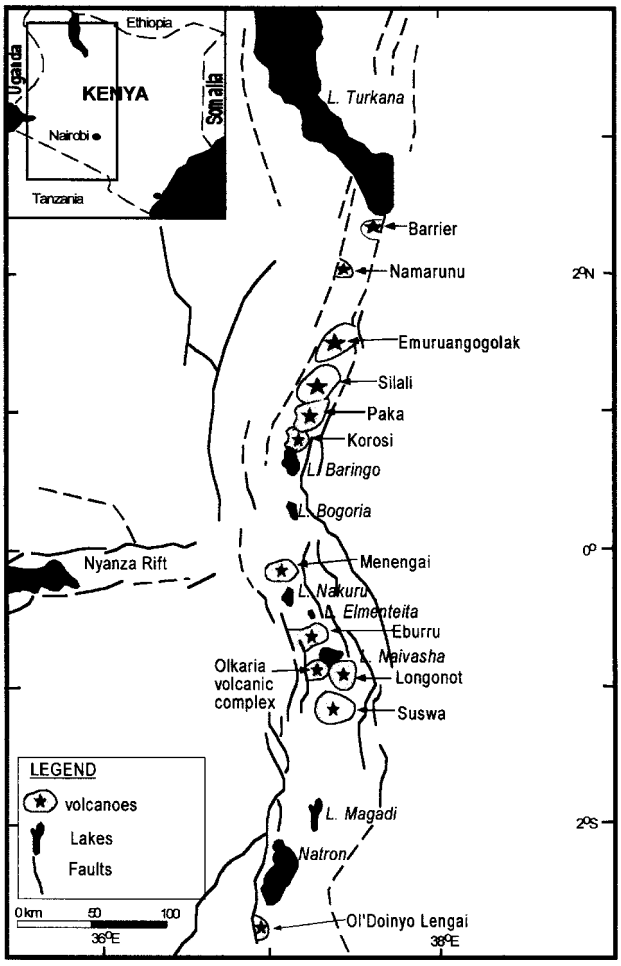

FIGURE 1: Map of the Kenya rift faults showing the major Quaternary central volcanoes and location of the Olkaria volcanic complex (KenGen 1999)

various bilateral and multilateral agreements. The exploration work identified Olkaria to be suitable for geothermal prospecting. By 1976, six deep wells had been drilled and in 1981 the first 15 MWe generating unit was commissioned. More wells were drilled and connected to the steam gathering system. Unit 2 and Unit 3, each 15 MWe, were commissioned in 1982 and 1984, respectively. Currently twenty-three wells are connected to the steam gathering system. Some of the shallow wells initially connected to the steam gathering system have since been retired. Six make-up wells have been drilled and four of these are already connected to the steam gathering system. The power plant produces the installed capacity of 45 MWe.

The Greater Olkaria geothermal area covers approximately 140 km^2 as shown in Figure 2. It is divided into seven fields, namely: Olkaria East, Olkaria Northeast, Olkaria Central, Olkaria Northwest, Olkaria Southwest, Olkaria Southeast, and Olkaria Domes (Mwangi, 2000). Each of the fields has been explored either partially or completely. The completely explored fields are Olkaria East, with a 45 MWe power plant, Olkaria Northeast, whose 64 MWe power plant is under construction and Olkaria Southwest (owned and operated by Orpower4 Inc.) with an 8 MWe combined cycle binary power plant in operation. Expansion of the power plant to 64 MWe or more is under way.

Currently, more than ninety-five (95) wells with varying depths (150-2500 m), have been drilled, and, hence, a large database of well information is available to assist in understanding the reservoir.

The objective of this research project is to re-evaluate some geochemical data from nineteen wells selected to represent all the sectors of the Greater Olkaria geothermal area with a view of getting a better understanding of the fluid compositions in the producing aquifers.

The geochemistry of each individual field has earlier been reported - Olkaria West (KPC 1984, 1990; Muna 1990; Wambugu 1995), Olkaria Northeast (KPC 1988; Wambugu 1996), Olkaria East (Muna 1982; KPC, 1982a, 1982b, 1984, and 1988; Karingithi 1992, 1993, and 1996) and Olkaria Domes (Karingithi 1999). From the above references, it can be concluded that the reservoir chloride concentration is declining through the different fields in the order: Olkaria Northeast field (ONEF) - Olkaria East field (OEF) - Olkaria West field (OWF) - Olkaria Domes field (ODF). The aquifer chloride concentration for each field in descending order is 300-550, 170-700, 100-500, and 180-270, for ONEF, OEF, OWF, and ODF, respectively. Figure 3 shows the distribution of the total discharge Cl concentration in Olkaria. It should be noted that the data used for comparison was the initial chemical data for the OEF before production. By considering the most recent data, the values in the OEF are seemingly higher than in the other fields.

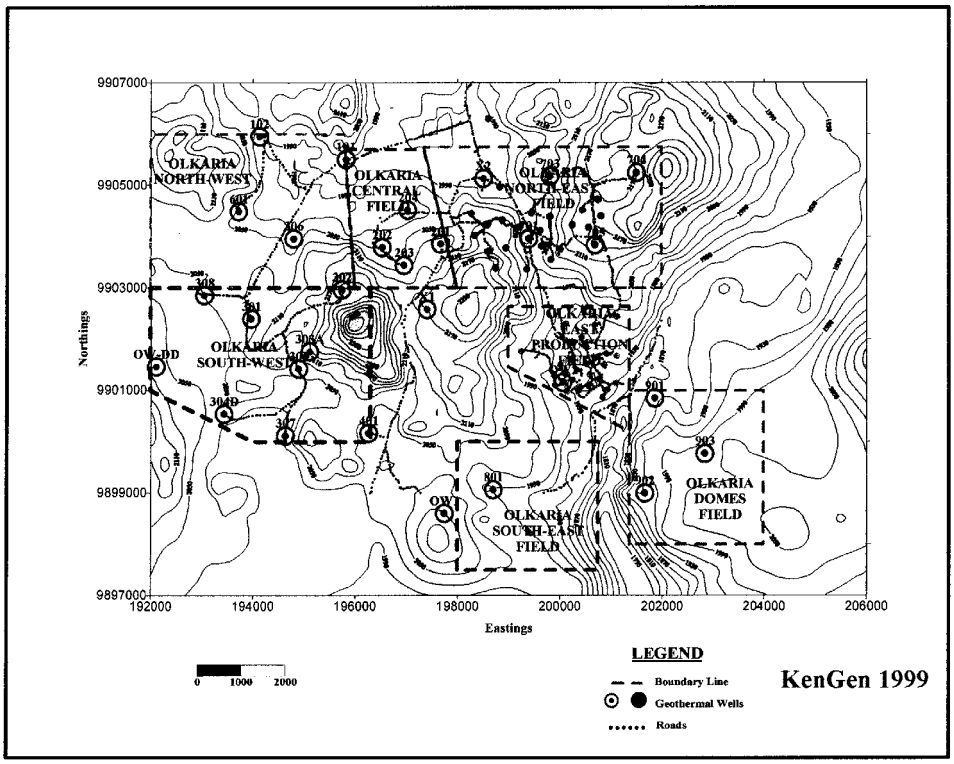

FIGURE 2: Geothermal fields within the Greater Olkaria geothermal area (KenGen 1999)

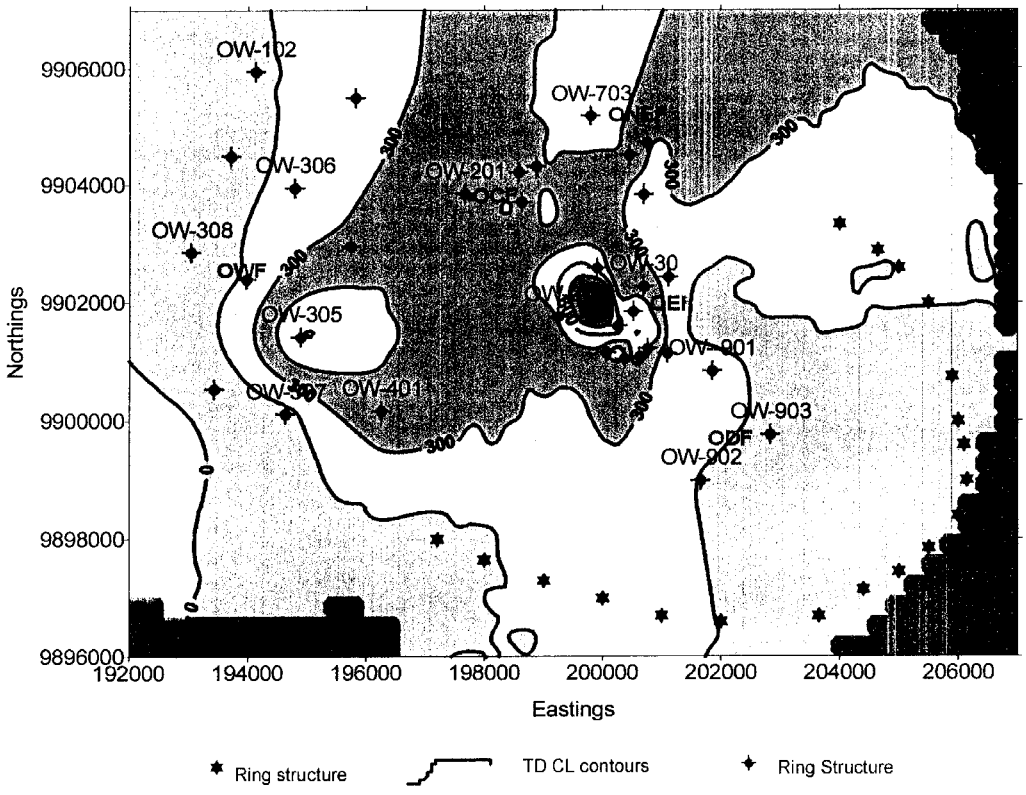

FIGURE 3: Total discharge Cl concentration distribution in Olkaria (KenGen 1999)

TABLE 1: Chemical analysis results of water samples for selected Olkaria wells, the samples were collected at the weirbox. Concentrations are in ppm (mg/kg)

Well no.	WHP (bars)	Enth (kJ/kg)	Cond (µS/cm)	CO_2	H_2S	B	SiO_2	Na	K	Mg	Ca	F	Cl	SO_4	Al	Fe	pH	Li
OW-10	5.02	2535	4033	114.19	0.91	8.03	638	855.1	129.7	0.176	3.91	81.1	1080	57.0	0.985	0.099	8.75	0.99
OW-15	5.61	1899	3815	72.07	2.60	8.73	604	708.9	115.4	0.040	1.67	62.4	1040	40.6	0.824	<0.02	8.69	1.69
OW-16	5.86	1384	2509	82.86	2.06	5.42	573	481.5	69.0	0.047	1.01	69.6	636	35.9	0.686	<0.02	8.97	0.88
OW-19	5.32	1823	2523	65.47	9.48	8.85	622	527.3	93.5	0.032	1.08	63.8	700	39.2	1.048	<0.02	9.10	1.62
OW-23	6.11	2191	1661	131.93	7.88	4.03	653	369.9	52.0	0.051	0.90	74.8	221	42.4	0.710	0.037	9.44	0.70
OW-25	6.43	2516	2579	149.57	2.12	5.47	641	522.0	94.5	0.106	1.20	70.1	671	28.4	0.511	<0.02	9.15	1.00
OW-202	5.20	1104	3540	1245.65	2.38	2.50	320	743.0	128.0	0.040	0.79	53.4	354	75.0	0.858	<0.02	9.30	3.00
OW-301	7.39	1653	6482	2465.38	3.96	6.77	855	1282.7	208.2	0.066	0.66	104.8	240	112.0	0.666	<0.02	8.67	3.67
OW-302	5.66	1234	3879	578.16	3.43	3.54	744	632.6	101.2	0.082	1.04	76.9	505	54.4	0.784	<0.03	9.72	3.21
OW-304D	3.90	1672	3194	1751.97	0.97	3.33	364	959.4	73.6	1.732	3.48	23.8	52	92.9	0.521	0.139	8.13	0.65
OW-306	3.99	1037	2854	1080.93	2.90	6.26	551	850.0	96.4	0.081	1.20	61.7	251	50.4	1.375	0.091	9.15	0.96
OW-307	0.35	435	4314	1553.26	3.49	2.04	312	837.7	90.4	0.053	0.71	57.4	109	115.1	0.580	<0.03	9.22	1.35
OW-308	6.30	2049	12068	9657.51	0.18	3.38	307	2530.1	244.1	0.294	1.84	77.2	109	140.8	0.058	0.159	8.10	6.89
OW-709	7.06	1921	4415	318.03	6.54	5.13	649	845.7	217.7	0.037	1.41	28.0	770	72.6	0.892	<0.02	9.93	1.41
OW-714	14.92	1303	3532	135.02	8.44	3.63	739	557.1	108.0	0.056	0.88	66.4	682	35.2	1.053	0.014	9.54	1.51
OW-719	8.02	1259	2865	162.31	4.46	4.77	588	535.8	80.5	0.042	1.09	46.1	544	82.9	1.511	<0.02	9.38	1.02
OW-901	4.26	1854	2805	565.56	18.30	2.42	529	505.8	56.5	0.029	0.72	80.1	280	123.8	0.683	0.028	9.80	2.66
OW-902	3.15	1108	2262	433.83	2.00	1.50	477	447.8	41.4	0.049	1.31	51.5	212	99.9	2.117	0.083	9.55	1.59
OW-903	4.01	953	2433	633.72	3.51	1.11	443	493.0	47.0	0.036	0.71	45.7	178	102.9	1.224	<0.02	9.43	2.41

2. GEOLOGICAL AND GEOTHERMAL FEATURES OF THE RESERVOIR

2.1 Geology and stratigraphy

The Olkaria volcanic complex (Figure 4) is one of several major volcanic centres in the Central Kenya Rift of the East African Rift system, associated with an area of Quaternary silicic volcanism (Muchemi, 1999; Omenda 1998). The evolution of the Central Kenya Rift stress field and the resultant faults have been discussed by Strecker, et al. (1990). A structural N-S running boundary passes through the Olkaria Hill that divides the Greater Olkaria area into east and west stratigraphic zones. In the Olkaria area the surface to about 1400 m a.s.l. is covered by Quaternary comendites and pantellerites and an extensive cover of pyroclastic fall from Longonot and Suswa. Volcanic eruption centres are structurally controlled. The main centres are the Olkaria Hill, Ololbutot fault zone and the Gorge Farm area. The most recent volcanism is associated with the Ololbutot fracture zone. The youngest lava is the Ololbutot rhyolite flow, which is about 250 ±100 years BP (Omenda, 1998; Clarke et al., 1990).

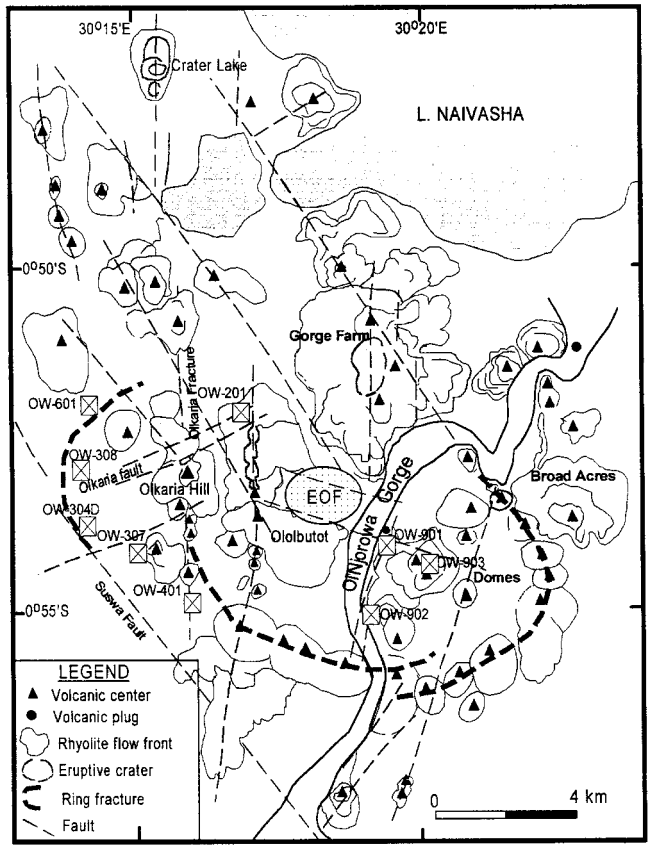

FIGURE 5: Volcano-tectonic map of the Greater Olkaria geothermal area (KenGen, 1999)

The subsurface geology of the Olkaria geothermal field can be divided into five broad lithostratigraphic groups based on age, tectono-stratigraphy, and lithology. The formations are: (1) The Mau tuffs; (2) Plateau trachytes, (3) Olkaria basalts and (4) Upper Olkaria volcanics insluding minor intrusives, as shown in Figure 5 (Muchemi, 1999; Omenda, 1998). The geothermal reservoir to the east of the Ololbutot fracture zone is hosted within the Pleistocene plateau trachytes while in the west it is within the Pliocene Mau tuffs.

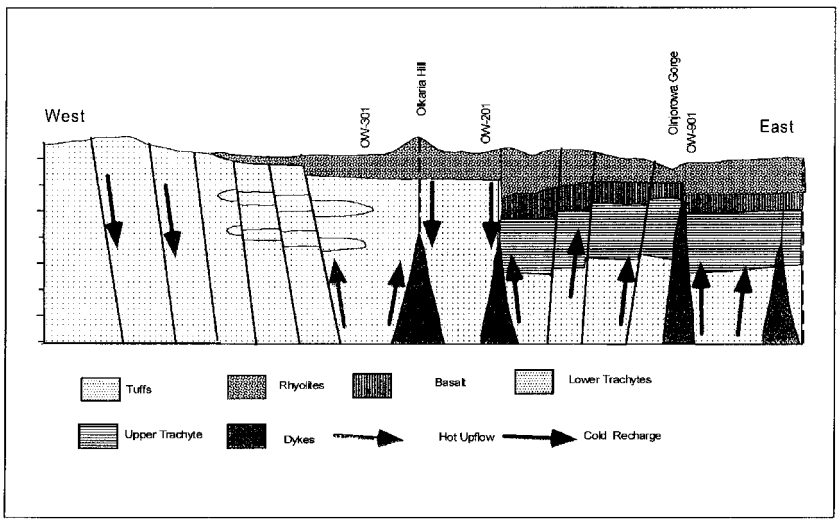

FIGURE 6: E-W geological cross-section through the Olkaria area (Muchemi, 1999; Omenda, 1998)

The regional structures in the area are represented by the Gorge Farm fault, the Suswa lineament and the east-northeast trending Olkaria fault zone (Muchemi, 1999). The main recharge paths to the Greater Olkaria geothermal area are NNW-SSE and NW-SE dipping major rift faults exposed on the Mau escarpment.

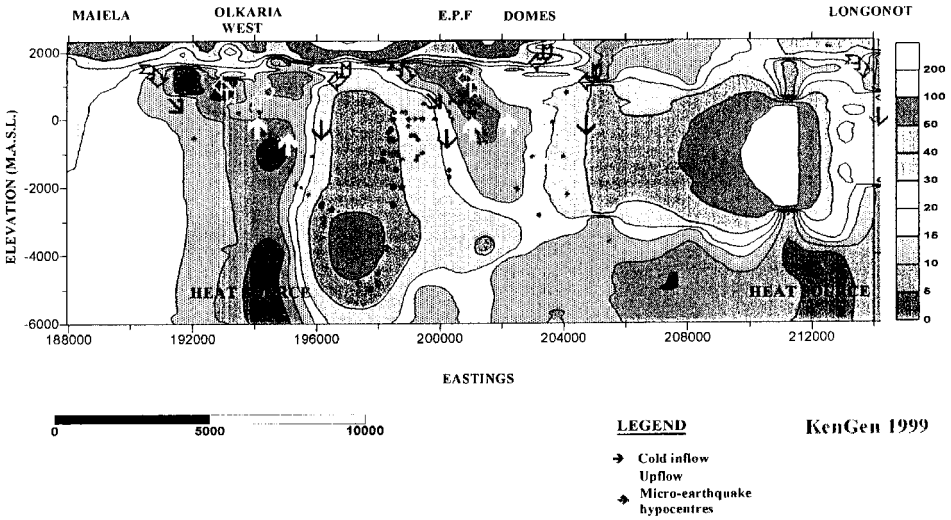

FIGURE 7: Integrated geophysical section from the Mau escarpment to Longonot through the Greater Olkaria geothermal area, resistivity in Ωm (KenGen, 1999)

Reactivated N-S rift floor faults and fractures control axial groundwater flow through the geothermal system, but have a shallower influence than the major rift forming faults that provide deep recharge.

The main structures controlling fluid movement within the Greater Olkaria geothermal area are N-S, NW-SE, NNW-SSE, and ENE-WSW faults and a ring structure. The NW-SE trending faults are inferred from aerial photographs and Landsat images since an extensive pyroclastic cover masks the surface features. Seismic data indicate that there is active movement along some of these faults (Simiyu et al., 1997). Clarke et al., (1990) and Mungania (1992) have demonstrated that most of the recent lava flows are associated with the N-S striking faults and the ring structure. These faults are thought to have numerous dyke swarms below the surface. Some of the dykes are well exposed in the Ol Njorowa gorge. Influence of the reactivated N-S rift floor faults and fractures on reservoir characteristics is shown by the temperature inversions that are common in most wells drilled close to the exposed N-S faults, e.g. wells OW-1, OW-201, and OW-401 (Omenda 1998).

Resistivity studies have been carried out by various workers since the early seventies (KenGen, 1999). The most notable finding is that the Olkaria West is different from the East and Northeast fields. Figure 6 shows the integrated geophysical model based on a combined interpretation of Transient Electromagnetic (TEM), DC-Schlumberger, and Magnetotelluric (MT) soundings within the area. The data show that the low-resistivity anomalies are controlled by linear structures running NE-SW and NW-SE. The resistivity is generally lower in Olkaria West than in the eastern Olkaria fields (KenGen, 1999).

2.2 Hydrothermal minerals

Muchemi (1999) and Omenda (1998) have summarized studies of hydrothermal alteration of rocks penetrated by wells drilled into the Olkaria geothermal system. Hydrothermal minerals present include kaolinite, biotite, hydrobiotite, vermiculite, chlorite, chlorite-illite, illite-smectite, smectite, epidote, calcite, quartz, fluorite, anhydrite Fe-oxides, prehnite, wairakite, stilbite, pyrite, adularia, albite, sphene, leucoxene, actinolite, garnet and talc. The most common secondary minerals are clay minerals, fluorite, anhydrite, calcite, pyrite and iron oxides. Clay mineral analysis shows that the prevailing clays in the east above 1000 m a.s.l., are smectite and chlorite, whereas in the west, illite is more dominant (Leach and Muchemi, 1987). At depths below 1000 m a.s.l., the dominant clay is interlayered chlorite-biotite and biotite. In general, the clay grading with depth in the east is smectite-chlorite-biotite and in the west smectite-illite-chlorite-biotite. Epidote has been observed to be closely associated with basalts and is more abundant in the eastern fields than in the western fields.

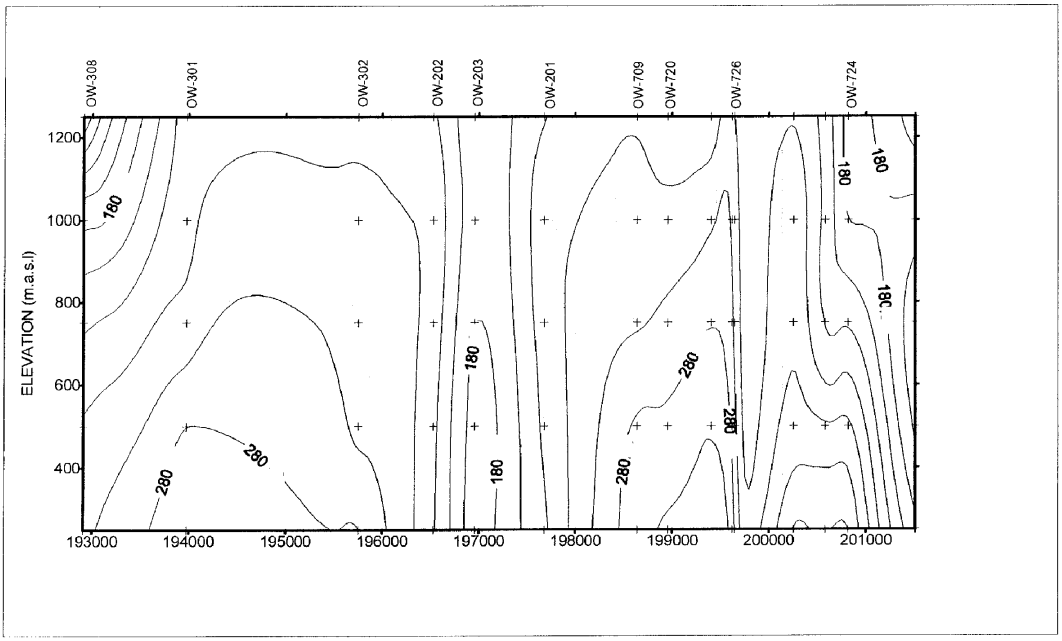

FIGURE 8: E-W temperature cross-section through the Olkaria area (KenGen, 1999)

2.3 Temperature and pressure

Temperature and pressure distribution across the entire field have been studied and indicate that fluid movement in the Olkaria geothermal area is associated with tectonic structures. The highest temperature recorded is 340˚C at 2000 m depth in well OW-19 in Olkaria East. The Olkaria East reservoir is two-phase, at least to the depth penetrated by the deepest wells. High temperatures are also observed in Olkaria West, Olkaria Northeast and Olkaria Domes while lower temperatures are observed in Olkaria Central (Figure 7). Pressures decrease both eastwards and westwards from respective peaks towards Olkaria Central. Within the Olkaria Central and Northeast, the pressures decline southward towards well OW-401 and Olkaria East, respectively (Ouma, 1999). The ENE-WSW trending Olkaria fault zone is the most important permeable structure in the entire Olkaria geothermal area. A permeability thickness (Kh) product of more than 10 Dm is common in the vicinity of this fault. The fault transects the Northeast and West fields, where it forms the most productive part of the system (Figure 4). This fault zone forms a hydrological divide. The geothermal reservoir in the north (including Olkaria Domes) is liquid-dominated and has no steam cap, whereas south of the fault the reservoir is a liquid-dominated two-phase system overlain by a steam dominated zone (Ambusso and Ouma, 1991; KenGen, 1999).

3. FLUID CHEMISTRY

3.1 Analytical data

A lot of chemical data have been collected from wells discharges at Olkaria over the years. Water samples have been collected from the weirbox at each wellhead. Steam samples from production wells in the Olkaria East production field were collected from the wellhead separators through a stainless steel sampling coil that was connected to the sampling point provided. From exploration and appraisal wells in other parts of the area, steam samples were collected from two-phase horizontal discharge pipelines with the aid of a webre separator. Sampling pressures for steam samples is variable but for water samples it is close to 0.8 bar-a. For the present study chemical data from 19 wells (Tables 1 and 2) have been used to study the state of mineral-solution equilibria in producing aquifers at Olkaria and to investigate the conformity between geothermometry temperatures and measured downhole temperatures at the level of permeable horizons in the selected wells.

TABLE 2: Average steam analysis results for selected Olkaria wells; concentrations are in mmoles/100 moles of steam in the steam samples

Well no.	Sampling pressure (bars)	CO_2	H_2S	H_2	O_2	CH_4	N_2
OW-10	4.53	142	7.87	6.37	1.31	1.11	6.24
OW-15	4.64	103	9.62	6.45	0.14	0.38	6.51
OW-16	4.66	111	11.16	5.65	0.01	0.43	2.90
OW-19	4.58	165	15.51	8.86	0.17	0.67	6.56
OW-23	5.04	146	13.13	9.53	0.12	0.31	4.49
OW-25	4.90	141	10.08	7.80	0.05	0.30	4.42
OW-202	1.46	280	1.00	0.02	0.07	0.50	1.57
OW-301	1.46	7675	6.40	1.90	0.00	1.47	20.30
OW-302	1.79	662	1.99	0.63	0.88	0.67	5.81
OW-304D	2.58	20650	4.76	1.69	0.00	3.05	31.26
OW-306	1.79	2048	5.23	0.97	0.00	1.69	14.12
OW-307	0.00	3027	4.82	4.38	83.65	2.23	382.24
OW-308	3.74	47812	0.91	0.05	9.30	4.08	50.17
OW-709	1.93	101	2.64	3.42	0.00	0.50	5.51
OW-714	2.76	146	7.89	2.22	0.00	0.60	6.05
OW-719	2.88	280	9.57	1.88	0.00	0.81	7.35
OW-901	1.56	336	8.91	4.36	0.19	0.55	9.30
OW-902	1.01	322	0.85	0.07	0.63	1.38	24.41
OW-903	1.26	501	1.87	0.35	1.19	1.29	34.21

The samples for which chemical data are presented in Tables 1 and 2 were collected in 1999. The analytical results for individual wells often show erratic time variations. Because the variations are erratic, it is considered that they may, at least, partly be due to analytical imprecision but not to natural variations. The numbers given for some components in Table 1 represent average concentrations for all samples collected from a particular well in cases where the 1999 samples gave values that departed significantly from the average.

The water discharged from wells in the Olkaria field is low in dissolved solids compared to water from most other drilled high-temperature geothermal fields in the world. Chloride concentrations in water at the weirbox range between 50 and 1100 ppm, being lowest in well OW-304D and highest in well OW-10. Water from wells in Olkaria East and Northeast tend to be highest in chloride. The high chloride concentrations observed for the Olkaria East and Northeast Fields could be the consequence of upflow of deep high-temperature geothermal fluid, although progressive boiling by heat flow from the rock may also contribute in the Olkaria East field. In the Olkaria West field the chloride concentrations are quite low (100–200 ppm) except in well OW-305, which discharges water similar to that discharged from the wells in the Olkaria East and Olkaria Northeast fields (530-750 ppm Cl at weirbox, Wambugu, 1995). Well OW-305 is thought to be tapping the up-flow fluid for Olkaria West field, while other wells are thought to discharge fluid, which has been diluted by either steam condensate or shallow groundwater.

The water from the weirbox of the Olkaria wells is slightly to moderately alkaline (pH 8.1-9.9 as measured at 20˚C) and is relatively high in bicarbonate, with 90-13000 ppm of HCO_3^-. The high bicarbonate is considered to be a consequence of CO_2 supply to the geothermal fluid and a subsequent reaction between the carbonic acid and minerals of the rock, which act like bases, thus converting some of the carbon dioxide to bicarbonate. The well discharges in Olkaria West are distinctly highest in carbon dioxide (Table 2). The CO_2 source is considered to be pre dominantly from the magma heat source of the geothermal system although carbon present in the rock may contribute a little.

Temperature reversals are observed in some wells, like OW-201 and OW-401. Some of the other recently drilled wells in Olkaria Central field, although not yet discharge-tested, indicate similar temperature reversals. These reversals could imply recharge of cold water encroaching the field from above or laterally. Such recharge could cause steam condensation, and reaction of the acid condensate could be the process leading to the formation of bicarbonate water rather than direct supply of CO_2 from the magmatic heat source to the deep, hot geothermal fluid.

From the relative abundance of chloride, sulphate and bicarbonate in the water from the weirbox of the Olkaria wells these waters would be classified as sodium-chloride and sodium-bicarbonate water, or mixtures thereof (Figure 8). Wells in the Olkaria East production field and in Olkaria Northeast discharge sodium-chloride type water. In Olkaria West they are, on the other hand, of the bicarbonate type. Wells in the Olkaria Central field discharge a mixture of chloride and bicarbonate end-member water as do wells in the Olkaria Domes area.

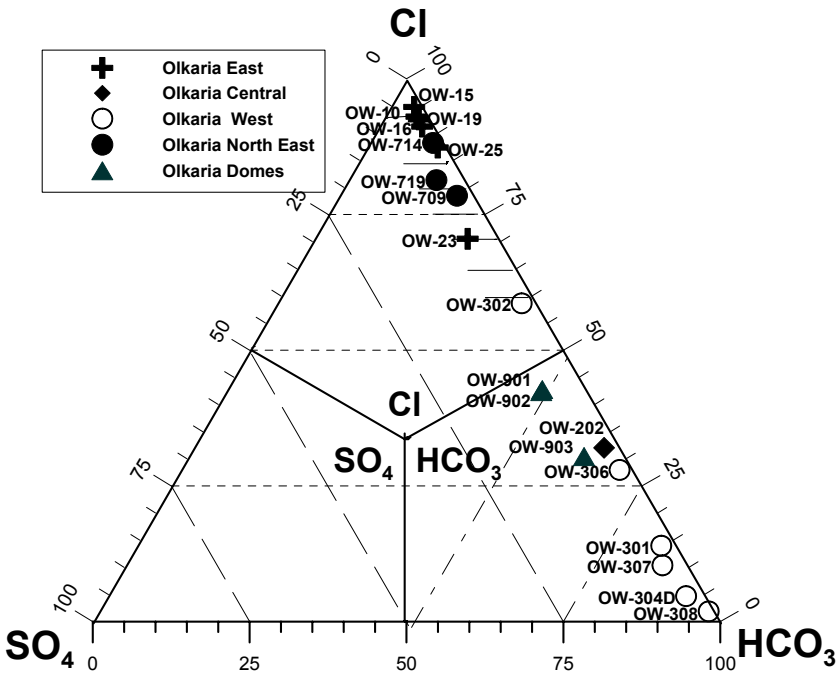

FIGURE 9: The Cl-SO_4-HCO_3 diagram for selected Olkaria geothermal well water samples

3.2 Isotope composition

Water samples collected from the wells and Lake Naivasha were analyzed for the stable isotopes oxygen-18 and deuterium. The results are shown in Table 3. Steam compositions were calculated from the data on the water samples assuming equilibrium between the two phases and using the α-isotope fractionation values reported by Henley et al. (1984). The aquifer isotopic compositions were calculated on the assumption that partial phase segregation in the depressurized zone around wells was responsible for the excess enthalpies, i.e., the steam fraction was taken to be equal to that produced by depressurization from the aquifer temperature to the weirbox. Quartz equilibrium temperature was taken as the aquifer temperature. A plot of deuterium versus oxygen-18 reveals interesting results (Figure 9). The samples plot close to the Kenya Rift Valley meteoric line (Kenya rainline - Clarke et al., 1990):

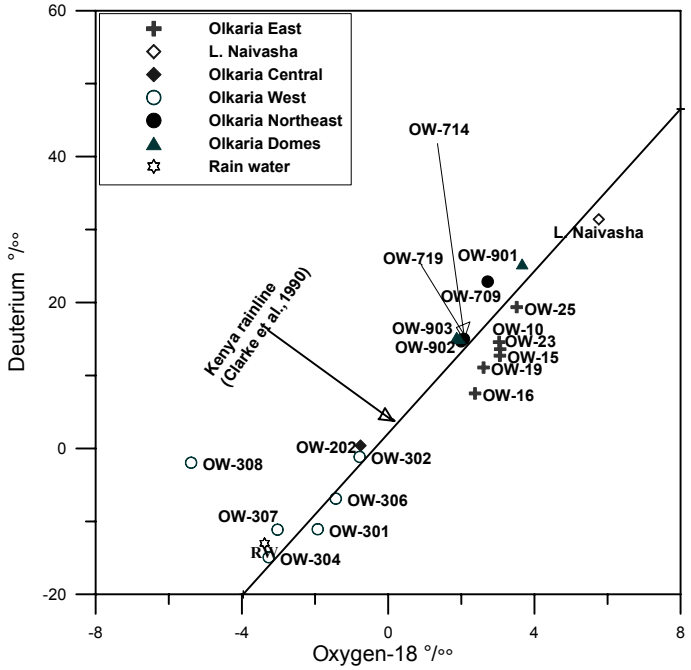

FIGURE 10: Stable isotope composition of samples from Greater Olkaria geothermal area

TABLE 3: Isotope composition of selected well water samples (weirbox and aquifer)

Location	Weirbox $\delta^{18}O$	Weirbox δD	Aquifer $\delta^{18}O$	Aquifer δD
OW-10	4.55	22.6	3.04	14.57
OW-15	4.37	19.7	3.05	12.72
OW-16	3.8	15.1	2.38	7.54
OW-19	4.1	19	2.61	11.09
OW-23	4.59	21.7	3.06	13.61
OW-25	5.03	27.4	3.52	19.37
OW-202	0.21	5.5	-0.75	0.38
OW-301	-0.16	-1.7	-1.93	-11.07
OW-302	0.87	7.6	-0.78	-1.16
OW-304	-2.21	-9.3	-3.27	-14.92
OW-306	-0.04	0.5	-1.43	-6.89
OW-307	-2.02	-5.8	-3.03	-11.14
OW-308	-4.55	2.5	-5.39	-1.96
OW-709	4.18	30.6	2.72	22.86
OW-714	3.71	23.7	2.07	15.00
OW-719	3.43	22.3	1.99	14.68
OW-901	4.97	32.2	3.67	25.28
OW-902	3.22	21.8	1.95	15.05
OW-903	3.09	21.7	1.87	15.24
L. Naivasha	1.95	31.40		
Rain water	1.87	-13.00		

$\delta D = 5.56\ \delta^{18}O + 2.04$ Kenya Rift Valley meteoric line.

The equation has a smaller slope than the world meteoric line proposed by Craig (1961):

$\delta D = 8\ \delta^{18}O + 10$ World meteoric line.

From Figure 9, it is seen that the Olkaria East samples cluster together 10 ± 5 δD ‰ and 3 ± 1 $\delta^{18}O$ ‰; Olkaria Northeast and Olkaria Domes samples plot within the same range but on the other side of the Kenya Rift Valley meteoric line. The samples from Olkaria West and Central plot together, $\delta^{18}O$ ranging from -0.75 ‰ to -5.4 ‰, the δD from 0.38 ‰ to -14.92 ‰. One sample is depleted with respect to $\delta^{18}O$, probably due to the high CO_2 in the geothermal system in Olkaria West and its vicinity. As CO_2 bubbles through the geothermal system, there is a preferred uptake of ^{18}O atoms, thus depleting the reservoir fluid of the same. Water from the eastern Olkaria sector, i.e. east of the Ololbutot fault, is enriched in both deuterium and oxygen-18 relative to local precipitation and as this water falls on or close to the local meteoric line, this indicates that the water evaporated before infiltrating into the bedrock of the geothermal system. The lower (more negative) deuterium values of the aquifer water in Olkaria West and Central indicate a different source (recharge area) for the Olkaria western sector, on one hand, and the eastern sector, on the other.

4. DATA HANDLING

4.1 Calculation of aquifer fluid compositions

Most of the wells at Olkaria have excess enthalpy, i.e. the enthalpy of the discharged fluid is higher than that of steam-saturated water at the respective aquifer temperature. Excess enthalpy may be the consequence of several processes. It may be a reflection of the high enthalpy of two-phase aquifer fluid. Alternatively, it could be caused by transfer of heat to the fluid flowing into wells from the rock in the depressurization zone around wells or by partial phase segregation of the water and steam in this zone (Arnórsson et al., 1990). All of these processes may be operative. Difficulties in evaluating their relative abundance lead to uncertainties as to how to calculate the chemical composition of the aquifer fluid from analytical data on water and steam samples collected at the wellhead.

To obtain a common reference point for the samples collected from wells discharging through a twin silencer to the atmosphere, component concentrations in water and steam were calculated at 10 bar-a vapour pressure with the aid of the WATCH- program (Arnórsson et al., 1982; Bjarnason, 1994). For the samples collected from production wells, the steam component concentrations were first recalculated to 1 bar-a, which was the sampling pressure of the water component, and subsequently the composition of both phases was recalculated at 10 bar-a. The aquifer chemistry was then recalculated using the compiled data. The enthalpy of saturated steam varies with temperature. It reaches maximum around 235˚C. In the range 180-270˚C (10-55 bar-a vapour pressure) it has a value close to this maximum, but at lower and higher temperatures it drops. As a consequence of this, the steam to water ratio (enthalpy) of a fluid has little effect upon evaporation of the water during depressurization in the pressure interval 10-55 bar-a but at lower and higher pressures water evaporation by depressurization increases with increasing steam fraction of the fluid. Most of the Olkaria wells have aquifer temperatures of less than 270˚C so enhanced water evaporation above 270˚C due to excess enthalpy can be ignored. On the other hand, the excess enthalpy may significantly enhance evaporation of water flowing into the weirbox, particularly for exploration and appraisal wells that do not have a steam wellhead separator. This is the reason for selecting the common reference point of 10 bar-a vapour pressure because it is not sensitive to variations in the excess of well discharge enthalpy.

Individual component concentrations have been calculated for the total discharge of the wells. For high-enthalpy wells, silica concentrations are variable and low. They decrease within increasing discharge enthalpy and yield low quartz equilibrium temperatures. Chloride concentrations are also variable and low and, for each field, decrease with increasing discharge enthalpy. These results indicate that the excess enthalpy is not due to an increase by heat flow from the aquifer rock, to the fluid flowing into wells in the depressurization zone around these wells. Pressure logging indicates that the reservoir in the Greater Olkaria geothermal area is liquid-dominated in terms of volume except for the steam zone that caps the liquid reservoir in the Olkaria East production field. This leaves phase segregation in the aquifer as the most important process in generating excess enthalpy well discharges. Aquifer component concentrations have been calculated on the assumption that this process accounts solely for the excess enthalpy.

In detail the procedure for calculating the aquifer fluid compositions for exploration and appraisal wells was as follows: (1) Gas concentrations in steam were reduced, corresponding to boiling from the sampling pressure to atmospheric pressure, (2) The compositions of water and steam were calculated at 10 bar-a vapour pressure using the measured discharge enthalpy value, and finally, (3) the aquifer component concentrations were calculated at the selected aquifer temperature assuming no effect of the excess enthalpy on the vaporisation of the water phase. For the production wells in the Olkaria East production field, the aquifer component concentrations were calculated according to two models. The first involved calculation of the water phase component concentrations in the wellhead separators from data on water samples collected from the weirbox, adding steam and gas lost during boiling between wellhead separator and silencer. Subsequently, using the measured discharge enthalpy values, water and steam compositions were calculated at 10 bar-a vapour pressure from the information on these components in the wellhead

separator. Finally, aquifer water compositions were calculated from the derived data at 10 bar-a by assuming that any excess steam does not affect evaporation of the water during depressurization. Alternately, the aquifer chemistry was calculated from data on steam and water compositions at atmospheric pressure assuming liquid enthalpy. Such an assumption is similar to the assumption that excess enthalpy does not affect water evaporation during depressurization. By this alternate approach, water evaporation is overestimated between wellhead separator and silencer but underestimated between wellhead separator and 10 bar-a vapour pressure, at least for excess enthalpy wells. Both of the approaches, described above, for the Olkaria East production wells yield about the same aquifer chemistry. For the present study the alternate method was used.

4.2 Calculation of aqueous speciation and mineral saturation

Having derived a satisfactory model to calculate component concentrations in the producing aquifers beyond the depressurization zone around wells, the WATCH chemical speciation program was used to calculate individual aqueous species activities and mineral saturation in the initial aquifer fluid. The data base for these calculations is that presented by Arnórsson et al. (1982) except for gas solubility, Al-hydroxide and Fe^{+3}-hydroxide dissociation constants which were taken from Arnórsson and Andrésdóttir (1999) and Diakonov et al. (1999).

The activity products for the following minerals were calculated: albite (low), microcline, calcite, anhydrite, prehnite, fluorite, epidote, pyrite, and pyrrhotite. The solubility constants for the same minerals, as a function of temperature, were obtained from the following sources: albite (low) and microcline (Arnórsson and Stefánsson, 1999; Arnórsson, 2000), calcite and fluorite (Arnórsson et al., 1982) and anhydrite, prehnite, epidote, pyrite and pyrrhotite (Gudmundsson and Arnórsson, 2001). Comparison between the solubility constant (K) and the activity product (Q) permits evaluation of whether the water is undersaturated ($Q<K$), at equilibrium ($Q=K$) or supersaturated ($Q>K$) with a particular mineral.

5. PRODUCING AQUIFER AND GEOTHERMOMETER TEMPERATURES

Permeable horizons in wells drilled at Olkaria have been identified by circulation losses during drilling and, in particular, by temperature logging during thermal recovery of the wells. The temperature of these horizons, where they intersect wells, have been inferred from temperature measurements after thermal recovery of the wells. The depth level of these horizons in the 19 wells specifically selected for this study and their temperatures (ranging from 175 to 310˚C) are shown in Table 4, together with several gas and solute geothermometer temperatures. The calibrations used for quartz, Na/K and Na/K/Ca solute geothermometers are those given by Fournier and Potter (1982), Arnórsson (2000) and Fournier and Truesdell (1973), respectively. For the gas geothermometers (CO_2, H_2S and H_2) the calibrations provided by Arnórsson and Gunnlaugsson (1985) were used. Two temperature values for each of the H_2S and H_2 geothermometers are shown in Table 4. One corresponds with calibration for water having <500 ppm Cl, and the other for water with >500 ppm Cl.

Conformity is rather good between the solute geothermometers. The difference between the quartz and Na/K geothermometer, on one hand, and the quartz and Na/K/Ca geothermometer, on the other, is illustrated in Table 5. The difference between the quartz and Na/K geothermometers does not portray any identifiable trends; the difference ranges between -66 and 30˚C for individual wells. The two extremes, 66 and 60˚C, are for wells OW-709 and OW-902. No explicit explanation can be given for this variance. On average the difference is 20˚C. The Na/K/Ca geothermometer yields, on the whole, systematically higher values than the quartz- and Na/K geothermometers, the difference with quartz being, on average, 27˚C. Correlation between quartz geothermometer temperatures and the other geothermometers considered in this study are illustrated in Figure 10 (A-F).

TABLE 4: Geothermometer temperatures (˚C) and measured aquifer temperatures

Well	H_2S (saline)	H_2 (saline)	CO_2	H_2S (dilute)	H_2 (dilute)	Qtz	Na/K	Na-K-Ca	Aquifer temp.	Depth level of aquifers (m)
10	257	285	211	186	225	247	242	254	255,260,270	750, 850,1150
15	262	286	196	197	228	229	250	266	245,265, 270	800, 1200-1300
16	269	287	213	207	229	239	236	253	240	950-1300
19	276	290	226	217	236	245	260	270	245,270	1000, 1500
23	270	292	222	209	239	248	234	246	245, 265,280	800,1000, 1200
25	262	287	210	196	230	247	262	270	260,270	800, 1400-1600
202	217	101	282	92	189	196	256	283	215, 230	1250, 1400-1600
301	257	273	523	185	197	269	250	292	265,275	1200, 1600-1850
302	239	263	309	143	166	259	248	267	245,270	1000,1400-1600
304D	251	271	810	172	190	205	179	213	250,265	1100-1300, 1600-1800
306	259	271	397	190	190	236	213	248	220,255	800,1500-1700
307	nd	nd	nd	nd	nd	200	208	252	175,230	750,1400-1650
308	218	249	272	92	111	184	198	258	165,220,225	1000, 1250,1400
709	238	283	206	140	222	242	308	310	250,275,310	1100, 1500, 1795
714	262	276	234	195	203	258	270	281	225,275,290	900-1100, 1500, 2000
719	259	279	260	190	211	240	241	258	220,260,290	750-1000, 1250,1800
901	282	313	234	224	271	228	212	240	250,280,305	900-1000, 1500-1700,
902	223	239	291	104	60	225	195	219	220,240,245	1000-1250, 1500-1600
903	299	243	358	239	84	220	197	230	215,220	950-1100, 1500-1600

TABLE 5: Differences between quartz and other geothermometers (˚C)

Well	Qtz-NaK	Qtz-CO_2	Qtz-H_2S saline	Qtz-H_2 saline	Qtz-H_2S dilute	Qtz-H_2 dilute
10	5	36	-10	-38	63	23
15	-21	33	-33	-57	47	16
16	3	26	-30	-48	31	10
19	-15	19	-31	-45	29	10
23	13	26	-23	-44	42	13
25	-15	37	-15	-40	53	19
202	-60	-86	-21	95	100	3
301	19	-254	12	-4	94	82
302	11	-50	20	-4	122	99
304D	26	-605	-46	-66	26	8
306	23	-161	-23	-35	45	
307	-8	-	-	-	-	-
308	-14	-88	-34	-65	92	73
709	-66	36	4	-41	105	23
714	-12	24	-4	-18	68	60
719	-1	-20	-19	-39	50	29
901	16	-6	-54	-85	3	-44
902	30	-66	2	-14	118	162
903	23	-138	-79	-23	-23	133

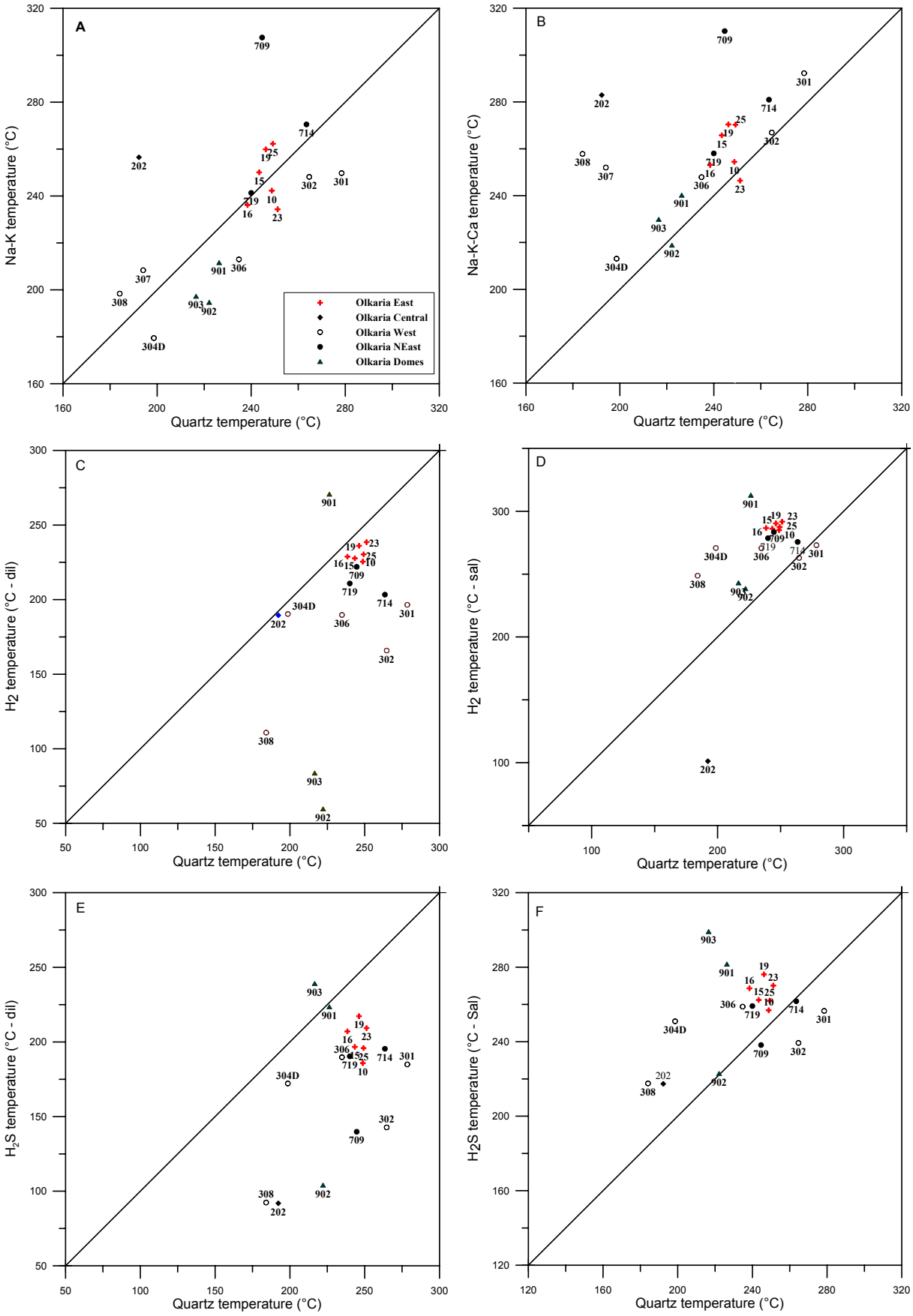

FIGURE 10: Correlation between quartz and various geothermometers

The calibration proposed by Arnórsson and Gunnlaugsson (1985) for "dilute" (<500 ppm Cl) and "saline" (>500 ppm Cl) water yields systematically low and high H_2S temperatures relative to quartz for most wells, or by 58 and 21˚C on average, respectively. The corresponding numbers for the H_2 geothermometer are 41 and 32˚C. Using the calibration for saline waters, the H_2S geothermometer temperatures range between 217 and 299˚C, well OW-202 having the lowest H_2S temperature and well OW-903 the highest. The H_2 geothermometer temperatures range between 101 and 313˚C, wells OW-202 again yielding the lowest value but well OW-901 the highest (Table 3). Using the gas calibrations for dilute water, the reverse is observed. The quartz geothermometer temperatures are, on the whole, much higher than the respective H_2S and H_2 temperatures. The difference varies from 3˚C to as much as 122˚C. For the wells in Olkaria East, Northeast and Domes, conformity is generally reasonable between the quartz and CO_2 geothermometers, but for Olkaria Central and Olkaria West the CO_2 geothermometer yields high and unrealistic values.

The gas geothermometers proposed by Arnórsson and Gunnlaugsson (1985) are geochemically calibrated, i.e. they involve correlating measured aquifer temperatures with the calculated concentrations of these gases in the aquifer water. Yet they considered that the mineral assemblage, calcite+quartz+epidote+prehnite, was likely to control aquifer water CO_2 concentrations and the mineral assemblage of pyrite+pyrrhotite+ epidote+prehnite both H_2S and H_2 aquifer water concentrations. Geochemical calibration was preferred, rather than a chemical thermodynamic one in view of rather poor quality of available chemical thermodynamic data on these minerals. Since the work of Arnórsson and Gunnlaugsson (1985) various chemical thermodynamic data assessments have led to improved quality of data on minerals involved in the mineral buffers mentioned above (Berman, 1988; Holland and Powell, 1990, 1998; Gottschalk, 1997). This led to theoretical calibration of all three gas geothermometers for epidote compositions in hydrothermally altered basalts. The compositions of all the minerals constituting the gas-mineral buffer are quite pure, except for epidote, of which the iron content varies with that of the host rock. Data are not available on epidote compositions at Olkaria that would permit theoretical calibration of the various gas geothermometers for that field. Evidently, a valid calibration for the Olkaria field is intermediate for the calibrations proposed by Arnórsson and Gunnlausson (1985) for "dilute" and "saline" geothermal waters.

The anomalously high CO_2 temperatures in Olkaria West and Olkaria Central could be the consequence of CO_2 control by a mineral buffer other than quartz+calcite+epidote+prehnite or that dis-equilibrium conditions prevail in the reservoir in these parts of the Olkaria field. Such dis-equilibrium conditions could be the consequence of CO_2 flux from a deep source in the geothermal system; from degassing of the magma heat source, even directly from the mantle (Omenda, 1998). A similar occurrence of anomalously high CO_2 temperatures has been observed in the Krafla geothermal area of Iceland, shortly after the initiation of a volcanic eruption period that started in 1975 and lasted until 1984. The increase in CO_2 was attributed to degassing of fresh magma intruded into the roots of the geothermal system (Ármannsson et. al., 1987).

From comparison between measured temperatures of aquifers (permeable horizons) and the solute geothermometer results, deductions have been made regarding which, if any of these horizons, dominate well discharges, Table 4. The results indicate that the shallowest horizons are usually the main or sole contributor to the discharge. These horizons may not be represented by horizontal layers but, at least in some cases, by vertical or near-vertical faults and fractures. In case of near-vertical permeable structures, a deeper aquifer could yield fluid into a well by downward movement of that fluid along these structures.

6. CALCULATION OF MINERAL SATURATION

The solubility product (Q) for each of the following hydrothermal minerals: albite (low), microcline, calcite, anhydrite, prehnite, fluorite, epidote, pyrite, and pyrrhotite, has been plotted as a function of temperature in Figure 11 (A-I). Also shown in the diagrams of this figure are the solubility constant curves for each mineral. Supersaturation is indicated when the solubility product (Q) values are higher than the solubility constant (K) values at a particular temperature, and undersaturation when $Q<K$.

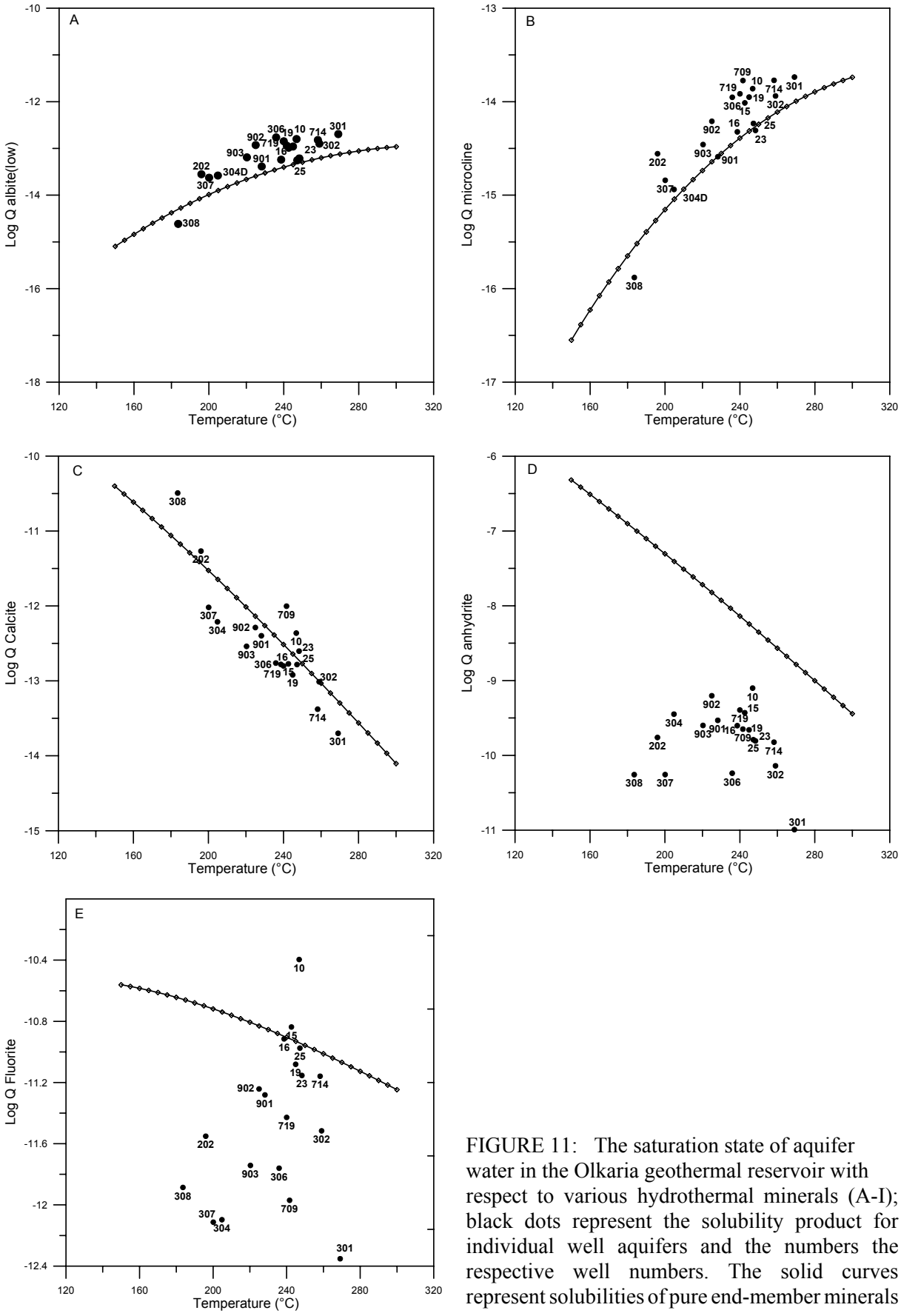

FIGURE 11: The saturation state of aquifer water in the Olkaria geothermal reservoir with respect to various hydrothermal minerals (A-I); black dots represent the solubility product for individual well aquifers and the numbers the respective well numbers. The solid curves represent solubilities of pure end-member minerals

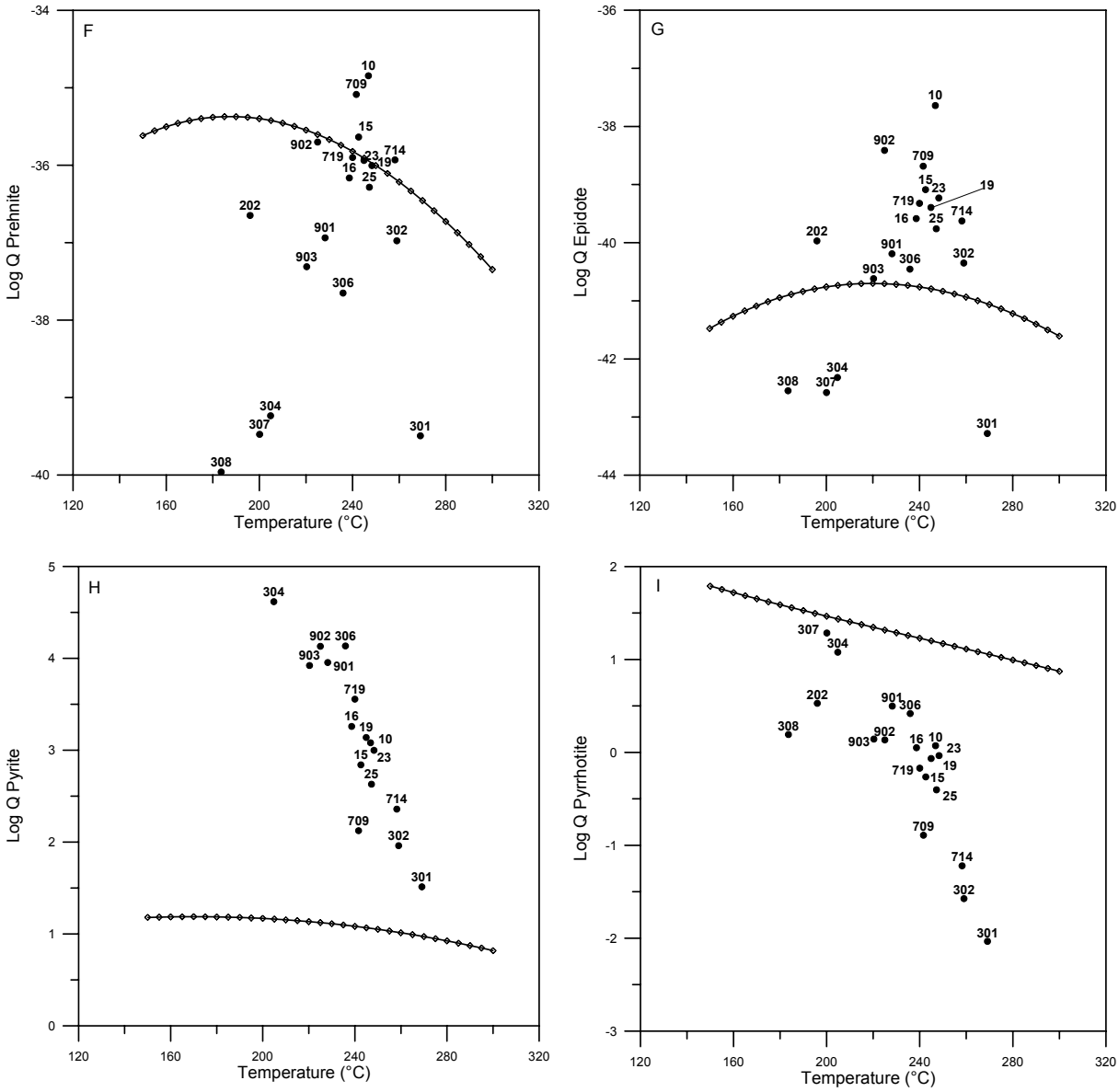

FIGURE 11: Continued (F-I)

6.1 Low-albite and microcline

The results depicted in Figures 11A and B indicate the aquifer water at Olkaria is saturated to slightly supersaturated with respect to low-albite (fully ordered albite with respect to Al and Si) and microcline (the stable K-feldspar at low temperatures). For low-albite the degree of supersaturation corresponds to 0.33 log Q units on average and 0.22 log Q units for microcline. The hydrothermal K-feldspar identified at Olkaria is adularia. According to calorimetric data (Hovis, 1988), the solubility of these two types of feldspars is practically the same. Therefore, the microcline solubility curve presented in Figure 11B can be taken to also represent adularia. The degree of low-albite and microcline supersaturation is not regarded as significant. There is some uncertainty involved in calculation of the aluminium speciation activities that affect the calculated log Q values. However, the predominant Al-hydroxide species in the water is $Al(OH)^{-}_{4}$, independent of which chemical thermodynamic data are selected: those of Castet et al. (1993), Pokrovskii and Helgeson (1995) and Arnórsson and Andrésdóttir (1999). In calculating the solubility products for the alkali feldspars, the Si-Al dimer (Pokrovski et al., 1998) was not considered. This dimer

may, according to the experimental results of Pokrovski et al. (1998) constitute a substantial fraction of the aqueous aluminium concentrations in geothermal water, about half for the Olkaria water, thus lowering the log *Q* values by about 0.3 log units for both low-albite and microcline, or quite close to the solubility constant curves. However, Stefánsson and Arnórsson (2000) have observed that a calculated saturation index for high-temperature geothermal water worldwide, for both low-albite and microcline, is generally negative (undersaturation) if the Si-Al dimer of Pokrovski et al. (1998) is taken into consideration. Their conclusion is that the stability of this complex may be overestimated, at least at high temperatures.

6.2 Calcite and cation/proton activity ratios

The results of Figure 11C indicate that most of the aquifer water is somewhat calcite undersaturated. The results indicate slight supersaturation for the aquifer water of wells OW-10, OW-709, OW-202 and OW-308 but undersaturation for the aquifer water of other wells. On average the departure from saturation is 0.13 log *Q* units and the standard deviation of the departure from equilibrium is 0.35 log *Q* units. Equilibrium with calcite is rapidly attained at high temperatures. For this reason it is to be expected that high-temperature geothermal water would be very close to being calcite saturated. However, in view of all the errors involved in sampling, analysis and assessment of the speciation of the aquifer water, departure in log *Q* from the calcite solubility constant curve of 0.3 is not regarded as significant. One of the main errors involved in calculating calcite saturation in the aquifer of wet-steam wells from data on the chemical composition of water and steam samples collected at the surface is the calculation of aquifer pH. One way of checking the reliability of the calculated aquifer pH value is to look at values obtained for the calcite saturation index and major cation/proton activity ratios. Too low an aquifer pH would show up as calcite undersaturation and low cation/proton activity ratios. At equilibrium with specific mineral buffers, geothermal water attains specific cation/proton activity ratios at a particular temperature (Arnórsson and Stefánsson, 2001). Figure 12 (A-D) depicts Na/H, K/H, $\sqrt{}$Ca/H and $\sqrt{}$Mg/H ion activity ratios. From this figure it is seen that Na/H, K/H and $\sqrt{}$Mg/H ratios are high relative to the equilibrium values proposed by Arnórsson and Stefánsson (2001). The samples with highest cation/proton ratios display the highest calcite supersaturation. On the other hand, $\sqrt{}$Ca/H ion activity ratios are low, particularly for the wells in Olkaria West.

The aquifer pH for most of the wells is around 6.5. However, the water in the aquifer of wells OW-202, OW-308 and OW-709 has a pH in excess of 7, and well OW-304D a value below 6. These wells have Na/H, K/H and Mg/H ion activity ratios, which depart much from the rest of the wells and the equilibrium values, as proposed by Arnórsson and Stefánsson (2001).

The relationship between the bicarbonate content of the geothermal water and the $\sqrt{}$Ca/H ion activity ratios suggest that the stability of the $CaHCO_3^-$ ion pair is overestimated in the WATCH speciation program with the result that a substantial part of the analyzed Ca concentrations in the water samples goes into forming this ion pair and little is left to form a free Ca ion. The value of the stability constant for $CaHCO_3^-$ used in the WATCH speciation program was estimated. Later experiments on calcite solubility (Plummer and Busenberg, 1982) indicate lower stability constant for this ion pair, or by 0.6-0.7 log K units in the range 200-300°C. Overestimation of the stability of the $CaHCO_3^-$ ion pair would lead to negative saturation index values (undersaturation) for calcite and low $\sqrt{}$Ca/H ion activity ratios are indeed observed.

The concentrations of bicarbonate are generally high in water discharged from Olkaria wells except for wells in the East production field. This high bicarbonate together with the pH of the water samples cause CO_2 partial pressures to be higher than that of the atmosphere. As a result, these samples will tend to degas when placed in an open beaker during measurement of pH and titration of the carbonate carbon. Such degassing will tend to give high pH readings and low carbonate carbon concentrations. It is

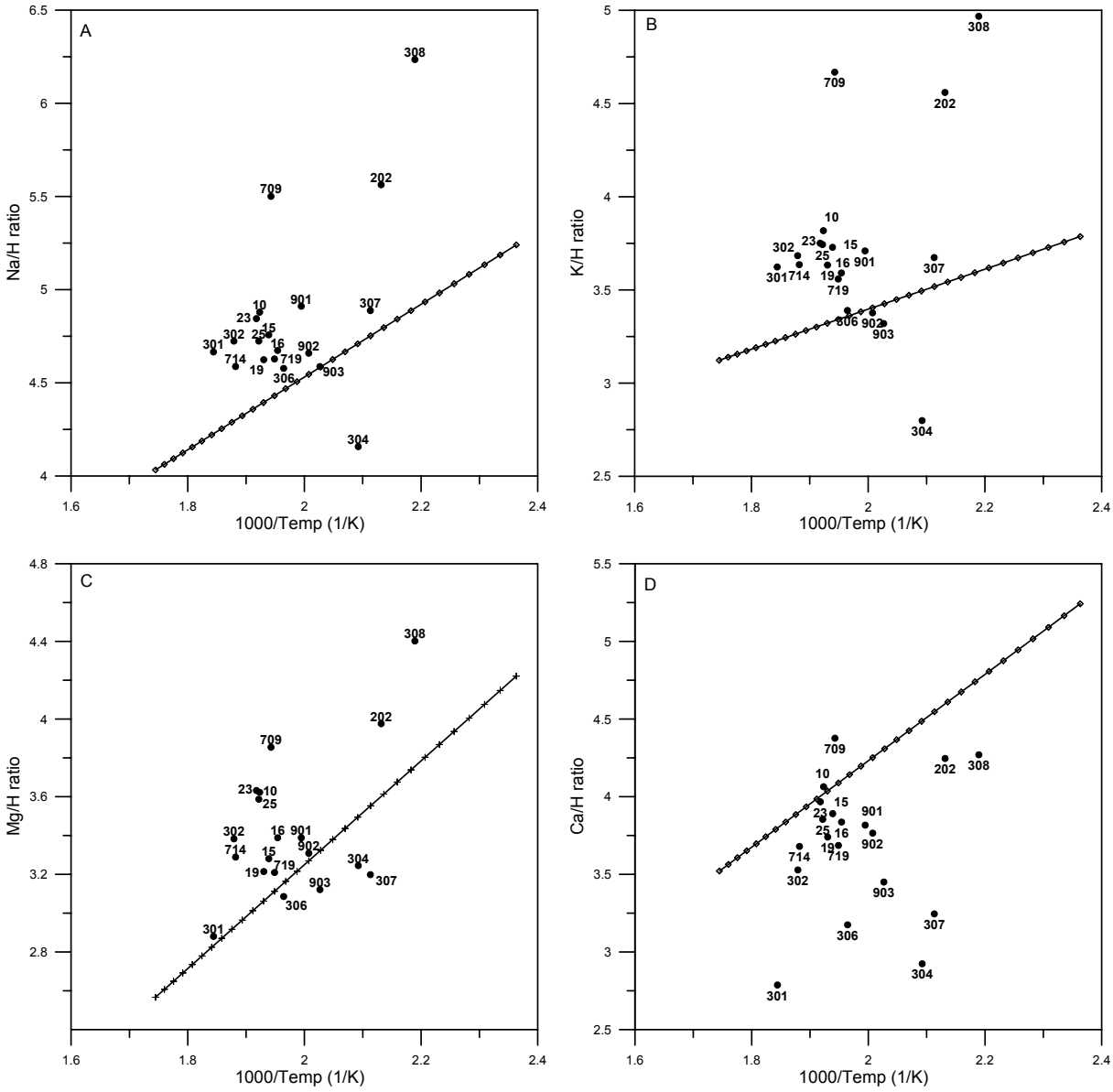

FIGURE 12: Cation/proton ratio variations with the reciprocal of the absolute temperature

considered that such degassing may be the cause of the observed high Na/H, K/H and √Mg/H ratios. It will also tend to give high √Ca/H ion activity ratios and calcite supersaturation. However, overestimation of the stability of the $CaHCO_3^-$ ion pair apparently has a larger effect in the opposite direction in the case of the √Ca/H activity ratio and calcite saturation.

6.3 Anhydrite and fluorite

The plot of the activity product for anhydrite and fluorite is shown in Figure 11D and E. All the water is undersaturated with respect to anhydrite, and saturated or undersaturated with fluorite. Both these minerals occur as hydrothermal minerals at Olkaria although anhydrite is confined to Olkaria West. There is, thus, inconsistency in the results. The cause for this inconsistency is considered to be the consequence of too low values for the dissociation constant of the $CaHCO_3^-$ ion pair leading to its too high stability and correspondingly too low values for the activity of the free calcium ion and too low log *Q* values for both anhydrite and fluorite. Additionally, some loss of calcium from solution by calcite precipitation in

the depressurization zone between undisturbed aquifer conditions and wellhead could contribute further to low calculated Ca^{+2} activity.

6.4 Prehnite and epidote

The log *Q* for the prehnite plot is shown in Figure 11F. Wells OW-10, OW-709, OW-15 and OW-714 are supersaturated with respect to prehnite. Their deviation from equilibrium follows the same order as given above. All the other wells discharge fluid that is to varying degrees, undersaturated with respect to prehnite. Extreme undersaturation is observed for wells OW-301, OW-304, OW-307 and OW-308. Epidote (Figure 11G) follows a similar pattern although the data points are on the whole shifted towards higher values. Some of the data points for Olkaria West and Central indicate undersaturation but others are close to saturation or indicate supersaturation. Decreasing iron content would lead to higher degree of supersaturation.

6.5 Pyrite and pyrrhotite

The results in Figures 11H and I indicate that all the Olkaria waters are pyrite supersaturated and pyrrhotite undersaturated. However, departure from equilibrium is not large when considering the uncertainty involved in the chemical thermodynamic data to calculate the ferrous iron speciation. It is concluded that the Olkaria aquifer waters are close to equilibrium with these sulphide minerals.

7. DISCUSSION

The calculated quartz equilibrium temperatures for wells depend on the model selected in accounting for the excess enthalpy in the well discharges. The model used in this study assumes that partial segregation of the water and steam phases in the depressurization zone around wells is responsible for the excess enthalpy. If heat flow from the aquifer rock to the fluid in the aquifer contributed to vaporisation of the water, the selected model would give high values for quartz equilibrium temperatures. It is considered that heat flow from the rock may contribute to the excess enthalpy of well discharges, particularly in the East production field, where reservoir pressure drawdown is most extensive but this process is not the dominant one in accounting for excess enthalpy. Calculation of quartz equilibrium temperatures by this model sometimes yields values that are lower than the temperatures at wellheads.

Mixing of fluid in wells from two or more aquifers of significantly different temperatures may lead to a discrepancy between various geothermometers. Such mixing leads to Na/K temperatures becoming higher than the quartz equilibrium temperatures, particularly if the hotter component in the mixture had higher salinity (Arnórsson, 2000). Extensive boiling causes initially calcite-saturated geothermal water to become supersaturated with this mineral and its deposition. For the low calcium and rich total carbonate carbon water at Olkaria, such calcite deposition may involve removal of a substantial part of the calcium from solution, resulting in too high Na/K/Ca temperatures. This process is thought to be the cause of high Na/K/Ca temperatures rather than faulty calibration of the geothermometer.

Contribution to well flow from two or more aquifers of significantly different temperatures causes H_2S temperatures to be higher that any solute geothermometer temperature, particularly if the deeper, hotter aquifer is rich in steam. Reliable calibration of the H_2S geothermometer is needed to study a possible discrepancy between the mentioned geothermometers. High H_2 temperatures, compared with those of H_2S, are indicative of the presence of equilibrium steam in the aquifer beyond the zone of depressurization. Again reliable calibration of the H_2 geothermometer is required to calculate the steam fraction in the aquifer (see Arnórsson et al., 1990). Yet, it appears that the gas geothermometer calibration for dilute water, given by Arnórsson and Gunnlaugsson (1985), provides reasonable results for the Olkaria

East production field where basalts are relatively abundant.

The aquifer water from the various parts of the Olkaria field, excepting the Olkaria East production field, are relatively rich in bicarbonate. The thermodynamic data in the WATCH speciation program on the dissociation constant for the $CaHCO_3^+$ ion pair is apparently too low, and lower than indicated by the experimental results on calcite solubility by Plummer and Busenberg (1982). This leads to too low calculated values for the activity of the free Ca^{+2} ion and correspondingly low solubility products (*Q*-values) for all calcium-bearing minerals such as calcite, anhydrite, fluorite, prehnite and epidote. To assess the saturation state of the reservoir water at Olkaria with respect to these minerals, it is necessary to update the data base in the WATCH speciation program with respect to the stability of the $CaHCO_3^+$ ion pair.

8. SUMMARY AND CONCLUSIONS

The solute geothermometers most often yield comparable aquifer temperatures for the wells specifically selected for the present study. They lie in the range 184 to 310°C, being lowest in well OW-308 and highest in well OW-709. Comparison between these temperatures and those measured at the depth level of the permeable horizons suggest that the shallowest horizons constitute the main feed zones for many of the wells. In order to obtain reliable results from the gas geothermometers, it is necessary to obtain appropriate calibration for these geothermometers that takes into account the composition of the mineral in the buffers with which these gases tend to equilibrate. The CO_2 gas geothermometer temperatures are erroneously high for Olkaria West, Olkaria Domes and in some wells in Olkaria Northeast. This is probably the result of lack of equilibration between CO_2 and the respective mineral buffer due to high flux of CO_2 from the magmatic heat source.

The oxygen-18 and deuterium isotope composition of water in producing aquifers at Olkaria plot close to the local meteoric line. In Olkaria West and Central, the isotope composition groups together. The δD varies from -18 to 0‰, while $\delta^{18}O$ varies from -6 to -1‰. Water in Olkaria East, Olkaria Northeast, and Olkaria Domes forms another group. The δD varies from 0.2 to 20‰. There exists a major difference between the fields to the west of Olkaria fracture and to the east of the Ololbutot fault, indicating that they have different recharge areas.

At quartz equilibrium temperature, the aquifer water has closely approached equilibrium, with some hydrothermal minerals, including low-albite, calcite and microcline. The water apparently is saturated to undersaturated with respect to fluorite, and somewhat undersaturated with respect to anhydrite. The apparent undersaturation may be an artifact due to erroneous data on the stability of the $CaHCO_3^+$ ion pair in the thermodynamic database of the WATCH speciation program.

ACKNOWLEDGEMENTS

Special thanks to my supervisor Stefán Arnórsson; I am honoured to have been his student. I would like to express my sincere gratitude to the UNU Staff - Dr. Ingvar B. Fridleifsson, Mr. Lúdvík S. Georgsson and Mrs. Gudrún Bjarnadóttir, for all the care, generous help and advice during the whole training period. I would like to thank the UNU, the Government of Iceland, Orkustofnun staff, and the KenGen management for granting me the opportunity to participate in the Geothermal Training Programme.

My deepest thanks to my family. This report is dedicated to them for all the sacrifice they made during the six months that I was away from home. All glory and honor to the Lord for the successful completion of the entire programme.

REFERENCES

Ambusso, W.J., and Ouma, P.A., 1991: Thermodynamic and permeability structure of Olkaria North-east geothermal field: Olkaria fault. *Geothermal Resources Council, Transactions, 15,* 237-242.

Ármannsson, H., Gudmundsson, Á., and Steingrímsson, B.S., 1987: Exploration and development of the Krafla geothermal area. *Jökull, 37*, 12-29.

Arnórsson, S., 2000: The quartz and Na/K geothermometers. 1. New thermodynamic calibration. *Proceedings of the World Geothermal Congress 2000, Kyotot-Tohoku, Japan,* 929-934.

Arnórsson, S., and Andrésdóttir, A., 1999: The dissociation constants of Al-hydroxy complexes at 0-350˚C and P_{sat}. *Proceedings of 5th International Symposium on the Geochemistry of the Earth´s Surface*, *Rotterdam, Balkema,* 425-428.

Arnórsson, S., Björnsson, S., Muna, Z.W., and Bwire-Ojiambo, S., 1990: The use of gas chemistry to evaluate boiling processes and initial steam fractions in geothermal reservoirs with an example from the Olkaria field, Kenya. *Geothermics, 19,* 497-514.

Arnórsson, S., and Gunnlaugsson, E., 1985: New gas geothermometers for geothermal exploration - calibration and application. *Geochim. Cosmochim. Acta, 49,* 1307-1325.

Arnórsson, S., Sigurdsson, S. and Svavarsson, H., 1982: The chemistry of geothermal waters in Iceland I. Calculation of aqueous speciation from 0˚C to 370˚C. *Geochim. Cosmochim. Acta, 46,* 1513-1532.

Arnórsson, S., and Stefánsson, A., 1999: Assessment of feldspar solubility constants in water in the range 0-350˚C at P_{sat}. *Am. J. Sci., 299,* 173-209.

Arnórsson, S., and Stefánsson, A., 2001: A novel way to demonstrate mineral-solution equilibria in groundwater systems. *Geofluids*, in press.

Berman, R.G., 1988: Internally consistent thermodynamic data for minerals in the system Na_2O-K_2O-CaO-MgO-FeO-Fe_2O_3-Al_2O_3-SiO_2-TiO_2-H_2O-CO_2. *J. Petrology, 29,* 455-522.

Bjarnason, J.Ö., 1994: *The speciation program WATCH, version 2.1.* Orkustofnun, Reykjavík, 7 pp.

Castet, S., Dandurand, J.L., Schott, J., and Gout, R., 1993: Boehmite solubility and aqueous aluminium speciation in hydrothermal solutions (90-350˚C): Experimental study and modeling. *Geochim. Cosmochim. Acta., 57*, 4869-4884.

Clarke, M.C.G., Woodhall, D.G., Allen, D., and Darling, G., 1990: *Geological, volcanological and hydrogeological controls on the occurrence of geothermal activity in the area surrounding Lake Naivasha, Kenya, with coloured 1:100 000 geological maps.* Ministry of Energy, Nairobi, 138 pp.

Craig, H., 1961: Isotopic variations in meteoric water. *Science, 133*, 1702-1703.

Diakonov, I.I., Schott, J., Martin, F., Harrichourry, J.C., and Escalier, J., 1999: Iron (III) solubility and speciation in aqueous solutions. Experimental study and modeling: part 1. Hematite solubility from 60 to 300˚C in NaOH-NaCl solutions and thermodynamic properties of $FE(OH)_4^-$(aq). *Geochim. Cosmochim. Acta, 63,* 2247-2261.

Fournier, R.O., and Potter, R.W. II, 1982: A revised and expanded silica (quartz) geothermometer. *Geoth. Res. Council Bull., 11-10*, 3-12.

Fournier, R.O., and Truesdell, A.H.,1973: An empirical Na-K-Ca geothermometer for natural waters. *Geochim. Cosmochim. Acta*, *37*, 1255-1275.

Gottschalk, M., 1997: Internally consistent thermodynamic data for minerals in the system SiO_2-TiO_2-Al_2O_3-Fe_2O_3-CaO-MgO-FeO-K_2O-Na_2O-H_2O-CO_2. *Europ. J. of Mineralogy, 9*, 175-223.

Gudmundsson, B.T., and Arnórsson, S., 2001: Secondary mineral - fluid equilibria in the Krafla and Námafjall geothermal systems, Iceland. *Applied Geochemistry,* (in press).

Henley, R.W., Truesdell, A.H., Barton, P.B. Jr., and Whitney, J.A., 1984: *Fluid - mineral equilibria in hydrothermal systems.* Reviews in Economic Geology, 1, 267 pp.

Holland, T.J.B., and Powell, R., 1990: An enlarged and updated internally consistent thermodynamic dataset with uncertainities and correlations: K_2O-Na_2O-CaO-MgO-MnO-FeO-Fe_2O_3-Al_2O_3-TiO_2-SiO_2-C-H_2-O_2. *J. Metamorphic Petrology, 8,* 89-124.

Holland, T.J.B., and Powell, R., 1998: An internally consistent thermodynamic data set for phases of petrological interest. *J. Metamorphic Petrology, 16,* 309-343.

Hovis, G.L., 1988: Enthalpies and volumes related to K-Na mixing and Al-Si order/disorder in alkali-feldspars. *J. Petrology, 29,* 731-763.

Karingithi, C.W., 1992: *Olkaria East production field geochemical report.* Kenya Power Company, Ltd., internal report, 96 pp.

Karingithi, C.W., 1993: *Olkaria East production field geochemical report.* Kenya Power Company, Ltd., internal report, 86 pp.

Karingithi, C.W., 1996: *Olkaria East production field geochemical report.* Kenya Power Company, Ltd., internal report, 124 pp.

Karingithi, C.W., 1999: *Olkaria Domes geochemical model.* The Kenya Electricity Generating Company, Ltd, internal report, 30 pp.

KenGen 1998: *Surface exploration of Kenya's geothermal resources in the Kenya Rift.* The Kenya Electricity Generating Company, Ltd, internal report, 84 pp.

KenGen 1999: *Conceptualized model of the Olkaria geothermal field (compiled by Muchemi, G.G.*) The Kenya Electricity Generating Company, Ltd, internal report, 46 pp

KPC, 1982a: *Programme for geochemical data collection and monitoring of well discharges prepared by Virkir Consulting Group Ltd.* Kenya Power Company, Ltd., internal report, 112 pp.

KPC, 1982b: *Status report on steam production, prepared by Merz and McLellan and Virkir Consulting Group Ltd.* Kenya Power Company, Ltd., internal report, 102 pp.

KPC, 1984: *Background report for scientific and technical review meeting.*Kenya Power Company, Ltd., internal report prepared by KRTA, 254 pp.

KPC, 1988: *Report on Olkaria and Eburru geothermal development.* Working papers on Northeast Olkaria, for STRM, Kenya Power Company, Ltd., internal report, 246 pp.

KPC, 1990: *Olkaria West field information report.* STRM, Kenya Power Company, Ltd., internal report, 240 pp.

Leach, T.M., and Muchemi G.G., 1987: Geology and hydrothermal alteration of the North and West exploration wells in the Olkaria geothermal field, Kenya. *Proceedings of the 9th New Zealand Geothermal Workshop, Geothermal Institute, Auckland,* 187-192.

Muchemi, G.G.,1999: *Conceptualised model of the Olkaria Geothermal Field.* The Kenya Electricity Generating Company, Ltd, internal report, 46 pp.

Muna, Z.W., 1982: *Chemistry of well discharges in the Olkaria geothermal field, Kenya.* UNU G.T.P. Iceland, Report 8, 38 pp.

Muna, Z.W., 1990: *Overview of the geochemistry of the Olkaria West geothermal field, Kenya.* Kenya Power Company, Ltd., internal report, 56 pp.

Mungania, J., 1992: *Geology of the Olkaria geothermal complex.* Kenya Power Company, Ltd, internal report, 38 pp.

Mwangi, M.N., 2000: Country update report for Kenya 1995-1999. *Proceedings of the World Geothermal Congress 2000, Kyoto- Tohoku, Japan,* 327-333.

Omenda, P.A., 1998: The geology and structural controls of the Olkaria geothermal system, Kenya. *Geothermics, 27-1*, 55-74.

Omenda, P.A., Onacha, S.A., and Ambusso, W.J., 1993: Geological setting and characteristics of the high temperature geothermal systems in Kenya. *Proceedings of the 15th New Zealand Geothermal Workshop, Geothermal Institute, Auckland,* 161-167.

Ouma, P.A., 1999: *Reservoir engineering report for Olkaria Domes field.* Kenya Electricity Generating Company Ltd., internal report, 54 pp.

Pokrovskii, G.S., Schott, J., Salvi, S., Gout, R., and Kubicki, J.D., 1998: Structure and stability of aluminium-silica complexes in neutral to basic solution. Experimental study and molecular orbital calculations. *Mineralogical Magazine, 62A,* 1194-1195.

Pokrovskii, V.A., and Helgeson, H.C., 1995: Thermodynamic properties of aqueous species and solubilities of minerals at high pressures and temperatures: The system Al_2O_3-H_2O-NaCl. *Am. J. Sci., 295,* 1255-1342.

Plummer, L.N., and Busenberg, E., 1982: The solubilities of calcite, aragonite and vaterite in CO_2-H_2O solutions between 0 and 90˚C, and evaluation of the aqueous model for the system $CaCO_3$-CO_2-H_2O. *Geochim. Cosmochim. Acta, 46*, 1011-1040.

Riaroh, D., and Okoth, W., 1994: The geothermal fields of the Kenya rift. *Tectonophysics, 236,* 117-130.

Simiyu, S.M., Mboya, T.K., Oduong, E.O., and Vyele, H.I., 1997: *Seismic monitoring of the Olkaria geothermal area, Kenya.* The Kenya Electricity Generating Company, Ltd., internal report, 62 pp.

Stefánsson, A., and Arnórsson, S., 2000: Feldspar saturation state in natural waters. *Geochim. Cosmochim. Acta, 64,* 2567-2584.

Strecker, M.R., Blisniuk, P.M., and Eisbacher, G.H., 1990: Rotation of extension direction in the Central Kenyan Rift. *Geology, 18,* 299.

Wambugu, J.M., 1995: *Geochemical update of Olkaria West geothermal field.* Kenya Power Company, Ltd., internal report, 40 pp.

Wambugu, J.M., 1996: Assessment of Olkaria-Northeast geothermal reservoir, Kenya based on well discharge chemistry. Report 20 in: *Geothermal Training in Iceland 1996*. UNU G.T.P., Iceland, 481-509.